Dynamic modeling of a midinfrared quantum cascade laser

A. Hamadou, S. Lamari, Jean-Luc Thobel

Journal of Applied Physics

Dynamic modeling of a midinfrared quantum cascade laser

Cite as: J. Appl. Phys. **105**, 093116 (2009); https://doi.org/10.1063/1.3124379
Submitted: 21 February 2009 • Accepted: 26 March 2009 • Published Online: 13 May 2009

A. Hamadou, S. Lamari and J.-L. Thobel

Dynamic modeling of a midinfrared quantum cascade laser

A. Hamadou,[1,a] S. Lamari,[2] and J.-L. Thobel[3]
[1]*Département de Génie Mécanique, Université Abdelhamid Ibn Badis de Mostaganem, Mostaganem 27000, Algeria*
[2]*Département de Physique, Université Ferhat Abbas de Sétif, Sétif 19000, Algeria*
[3]*Institut d'Electronique, de Microélectronique et de Nanotechnologie (IEMN), UMR 8520, Université Lille 1, Avenue Poincaré, BP 60069, 59652 Villeneuve d'Ascq Cédex, France*

(Received 21 February 2009; accepted 26 March 2009; published online 13 May 2009)

Based on a three-level rate equations model, we analyze through numerical simulations the population and photon number dynamics present within the cavity of a midinfrared quantum cascade laser. We find in particular that the injection current influences significantly the electron number dynamics trajectory. In addition, the equations that allow for the determination of the turn-on delay (t_{th}) and buildup (Δt) times are derived within the premises of our model in the most general case. The effects of the spontaneous emission factor β on Δt are also explored.
 [DOI: 10.1063/1.3124379]

I. INTRODUCTION

Quantum cascade (QC) lasers[1] are unipolar devices where the lasing process is assured by transitions between quantized energy levels within the conduction band. As opposed to conventional ones, QC lasers present a fundamental advantage residing in their characteristic property consisting in the control of the wavelength of the emitted light via the layer thickness rather than the band gap. This allows for the emission wavelength of such a laser to be changed at will without resorting to a different semiconductor. Up until now, various operating schemes for the QC laser have been put forward by different authors. Among the notable designs, the following can be mentioned: the three quantum wells active region scheme,[2,3] the superlattice active region design,[4,5] the two phonons active region one,[6] and the bound to continuum design.[7,8] Macroscopic theoretical modeling of the dynamics of a QC laser is complete once one knows the equations that govern the photon number in the cavity and the electron distribution among the different states involved.[9] On the other hand, one can also adopt a microscopic approach in modeling the carrier dynamics in these systems,[10–13] in such a case the need for phenomenological parameters is bypassed.

In a QC laser the delay time plays an important role that partly determines the device performance, in particular, it causes spontaneous emission induced intensity noise in the optical output power.[14] Equally as important for the QC laser operation is the turn-on delay time, that is the time needed for the laser to reach threshold. This time depends on the QC laser phonon scattering times and the injection current.

Our theoretical treatment laid below focuses only on the electrically injected three-level QC laser design proposed by Page *et al.*[2] where lasing takes place through transitions from the upper state (level 3) to the lower state (level 2), and the latter being subsequently depopulated by polar optical phonon emission into the ground state (level 1). Intersubband phonon scattering also occurs between levels 3 and 2, and 3 and 1, and is the main competing nonradiative process in midinfrared QC lasers. For details of the structure, we kindly refer the reader to the published literature.[2,15]

Our paper is organized as follows. Section I is a general introduction to the subject. Section II describes the model used to derive our results. Section III summarizes the salient features of our numerical results on the time evolution of the electron distribution among levels, the population inversion, as well as the photon number within the cavity. In addition, this section contains an analytical derivation of the turn-on delay and buildup times. Finally, Sec. IV concludes our paper and wraps up our main findings.

II. RATE EQUATIONS OF A MIDINFRARED QC LASER

Our investigation will focus on a three-level QC laser such as encountered in the literature[2,3] where the upper and lower states will be taken as levels 3 and 2, respectively, while the ground state used to empty the lower state through LO phonon emission will be called level 1. We will denote by N_1, N_2, and N_3 the respective instantaneous numbers of electrons in each of the three levels just alluded to and by N_{ph} the photon number of the cavity's one and only mode, the following rate equations then hold:

$$\frac{dN_3}{dt} = WL\frac{J}{e} - \frac{N_3}{\tau_3} - \Gamma\frac{c'\sigma_{32}}{V}(N_3 - N_2)N_{ph}, \tag{1a}$$

$$\frac{dN_2}{dt} = \left(\frac{1}{\tau_{32}} + \frac{1}{\tau_{sp}}\right)N_3 - \frac{N_2}{\tau_{21}} + \Gamma\frac{c'\sigma_{32}}{V}(N_3 - N_2)N_{ph}, \tag{1b}$$

$$\frac{dN_1}{dt} = \frac{N_3}{\tau_{31}} + \frac{N_2}{\tau_{21}} - \frac{N_1}{\tau_{out}}, \tag{1c}$$

$$\frac{dN_{ph}}{dt} = N\Gamma\frac{c'\sigma_{32}}{V}(N_3 - N_2)N_{ph} + N\beta\frac{N_3}{\tau_{sp}} - \frac{N_{ph}}{\tau_p}. \tag{1d}$$

In the above system of equations, J denotes the electron current density that tunnels into the upper level and e is the

[a]Author to whom correspondence should be addressed. Electronic mail: abd_hamado@yahoo.fr.

electronic charge, while W and L are the lateral widths of the cavity. Denoting by N and L_p the number of stages and length of each one of these, the whole volume V of the active area is then given by $NWLL_p$. In addition, in the above equations we introduced the mode confinement factor[16] Γ and the average velocity of light in the system c' given by $c'=c/n_{\text{eff}}$, where n_{eff} and c are the effective refractive index of the cavity and the speed of light in vacuum, respectively. The important parameter[17] β in Eq. (1d) defines the proportion of spontaneous emission events that emit a photon into the cavity mode whereas σ_{32} stands for the stimulated emission cross section between the upper and lower levels. The system dynamics is mainly determined by the three nonradiative scattering times denoted by τ_{32}, τ_{31}, and τ_{21} that are due to LO-phonon emission between the corresponding levels as well as the radiative spontaneous relaxation time τ_{sp} between levels 3 and 2. Furthermore, between two adjacent stages we model the escape of electrons by a rate $1/\tau_{\text{out}}$, where τ_{out} stands for the electron escape time. To complete the picture, we take into consideration the finite lifetime of the photon denoted by τ_p and given by $\tau_p^{-1}=c'(\alpha_w+\alpha_m)$, where α_w is the waveguide loss of the cavity while α_m is the mirrors loss expressed as $\alpha_m=-\ln(R_1R_2)/(2L)$, where R_1 and R_2 are the reflecting powers of facets 1 and 2, respectively.[16] For the sake of convenience, let us also introduce the lifetime τ_3 of the upper level which we write as

$$\frac{1}{\tau_3}=\frac{1}{\tau_{32}}+\frac{1}{\tau_{31}}+\frac{1}{\tau_{\text{sp}}}. \tag{2}$$

The radiative spontaneous emission relaxation time can be cast as follows:[18]

$$\frac{1}{\tau_{\text{sp}}}=\frac{8\pi^2e^2n_{\text{eff}}z_{32}^2}{\varepsilon_0\hbar\lambda^3}, \tag{3}$$

where ez_{32} is the dipole matrix element between states 3 and 2, ε_0 is the permittivity of vacuum, λ is the emission wavelength, and $\hbar$ is the reduced Planck constant. The stimulated emission cross section σ_{32} is given by[19]

$$\sigma_{32}=\frac{4\pi e^2z_{32}^2}{\varepsilon_0n_{\text{eff}}\lambda(2\gamma_{32})}, \tag{4}$$

where $2\gamma_{32}$ stands for the full width at half maximum of the electroluminescence spectrum.

In the steady state all the time derivatives in the rate equations given above vanish, an analytical solution of the system becomes then feasible and the following expressions for N_3 and N_2 ensue:

$$N_3=\frac{WL\frac{J}{e}\left(\tau_{21}\Gamma\frac{c'\sigma_{32}}{V}N_{\text{ph}}+1\right)}{\frac{1}{\tau_3}+\left(1+\frac{\tau_{21}}{\tau_{31}}\right)\Gamma\frac{c'\sigma_{32}}{V}N_{\text{ph}}}, \tag{5}$$

$$N_2=\frac{WL\frac{J}{e}\left(\frac{\tau_{21}}{\tau_{32}}+\frac{\tau_{21}}{\tau_{\text{sp}}}+\tau_{21}\Gamma\frac{c'\sigma_{32}}{V}N_{\text{ph}}\right)}{\frac{1}{\tau_3}+\left(1+\frac{\tau_{21}}{\tau_{31}}\right)\Gamma\frac{c'\sigma_{32}}{V}N_{\text{ph}}}. \tag{6}$$

The population inversion ΔN between the upper and lower levels as a function of the photon number N_{ph} can be then written as

$$\Delta N=\frac{WL\frac{J}{e}\tau_3\left(1-\frac{\tau_{21}}{\tau_{32}}-\frac{\tau_{21}}{\tau_{\text{sp}}}\right)}{1+\frac{N_{\text{ph}}}{N_{\text{ph,sat}}}}, \tag{7}$$

here we introduced the photon saturation number $N_{\text{ph,sat}}$ given by

$$N_{\text{ph,sat}}=\frac{1}{\tau_3\left(1+\frac{\tau_{21}}{\tau_{31}}\right)\Gamma\frac{c'\sigma_{32}}{V}}. \tag{8}$$

Making use of Eqs. (5), (7), and (8) in Eq. (1d), the following quadratic equation is then obtained for N_{ph}:

$$N_{\text{ph}}^2-\left[\left(\frac{J}{J_{\text{th}}}-1\right)+\frac{1}{\left(1+\frac{\tau_{21}}{\tau_{31}}\right)}\frac{\tau_{21}}{\eta_r}\frac{\beta}{\tau_{\text{sp}}}\frac{J}{J_{\text{th}}}\right]N_{\text{ph,sat}}N_{\text{ph}}-\frac{\tau_3}{\eta_r}\frac{\beta}{\tau_{\text{sp}}}\frac{J}{J_{\text{th}}}N_{\text{ph,sat}}^2=0, \tag{9}$$

where J_{th} denotes the threshold current density, which we define by equating the modal gain and the total losses that include those due to the mirrors and waveguide while the parameter η_r is the radiative efficiency given by

$$\eta_r=\frac{1-\frac{\tau_{21}}{\tau_{32}}-\frac{\tau_{21}}{\tau_{\text{sp}}}}{1+\frac{\tau_{21}}{\tau_{31}}}. \tag{10}$$

At threshold, we have

$$N\Gamma\frac{c'\sigma_{32}}{V}\Delta N_{\text{th}}=\frac{1}{\tau_p}, \tag{11}$$

where ΔN_{th} is obtained from Eq. (7) by setting N_{ph} to zero and making J_{th} replace J. After easy algebra, we get for J_{th} the following expression:

$$J_{\text{th}}=\frac{1}{\tau_3\left(1-\frac{\tau_{21}}{\tau_{32}}-\frac{\tau_{21}}{\tau_{\text{sp}}}\right)}\frac{L_p\varepsilon_0n_{\text{eff}}\lambda(2\gamma_{32})}{4\pi ez_{32}^2}\frac{(\alpha_w+\alpha_m)}{\Gamma}. \tag{12}$$

In Eq. (9), the last term can safely be dropped out and the photon number can then be obtained as

(i) below threshold ($J<J_{\text{th}}$),

$$N_{\text{ph,1}}\approx\frac{\tau_3}{\eta_r}\frac{\beta}{\tau_{\text{sp}}}\frac{1}{\left(\frac{J_{\text{th}}}{J}-1\right)}N_{\text{ph,sat}}, \tag{13}$$

(ii) above threshold ($J > J_{th}$),

$$N_{ph,2} \approx \left[\left(\frac{J}{J_{th}} - 1 \right) + \frac{1}{\left(1 + \frac{\tau_{21}}{\tau_{31}} \right)} \frac{\beta}{\tau_{sp}} \frac{\tau_{21}}{\eta_r} \frac{J}{J_{th}} \right] N_{ph,sat}. \quad (14)$$

The solution exhibited in case (i) is the trivial one and corresponds to a state where no laser oscillation takes place since $N_{ph} \approx 0$. Clearly the most interesting situation is that of case (ii) which shows that the photon number scales linearly with the current density J. Setting $N_{ph}=0$ and substituting J_{th} in Eq. (7) by its expression displayed in Eq. (12) we obtain the population inversion at threshold ΔN_{th} as

$$\Delta N_{th} = \frac{V}{N \Gamma c' \sigma_{32} \tau_p}. \quad (15)$$

Next using the theory developed above, we estimate numerically τ_p, σ_{32}, τ_{sp}, α_m, J_{th}, ΔN_{th}, $N_{ph,sat}$, and compute ΔN and N_{ph} for $J=2.5J_{th}$ using the following experimental QC laser parameters as reported in Refs. 2 and 15: $W=34$ μm, $L=1$ mm, $L_p=45$ nm, $R_1=R_2=0.29$, $\alpha_m=20$ cm^{-1}, $N=48$, $n_{eff}=3.27$, $z_{32}=1.7$ nm, $\tau_{32}=2.1$ ps, $\tau_3=1.4$ ps, $\tau_{21}=0.3$ ps, $\lambda=9$ μm, $2\gamma_{32}=12$ meV, and $\Gamma=0.32$. Our results are as follows: $\tau_p=3.36$ ps, $\tau_{sp}=38$ ns, $\sigma_{32}=1.8\times10^{-14}$ cm^2, $\alpha_m=12.4$ cm^{-1}, $J_{th}=3.33$ kA/cm^2, $\Delta N_{th}=8.5\times10^6$, $N_{ph,sat}=9.16\times10^8$, $\Delta N=8.5\times10^6$, and $N_{ph}=1.37\times10^9$. We note in passing the excellent agreement of our estimation for J_{th} compared to the reported[15] experimental value $J_{th}^{(exp)}=2.9$ kA/cm^2.

III. DYNAMICAL STUDY

A. Numerical analysis

In this section we explore the temporal evolution of the photon number N_{ph} and the population of levels N_1, N_2, and N_3. We carry this out by solving the system of nonlinear differential equations given in Eqs. (1a)–(1d) using a fourth order Runge–Kutta method with an integration step $h=0.1$ ps and the following initial conditions $N_1=N_2=N_3=N_{ph}=0$, the injection current J being finite and above threshold. The main features of our results are exhibited in Figs. 1–3.

In Fig. 1 we show the evolution of the electron number in the various levels as a function of time for different injection current strengths, the parameters used being those used in the previous section and are thus appropriate for cryogenic temperatures.[2,15] The different panels show first a very brief initial overshoot lasting roughly less than 1 ps followed by a regime where the distribution of electrons among the levels remains roughly constant, the system stays in this state for a period known as the buildup time Δt that is of the order of 30–146 ps depending on the value of the injected current: the higher the current the shorter the period. This stage corresponds to a very small number of photons, as time passes regardless of the current strength, the number of electrons in the upper level decreases before reaching its stationary value while populations of the lower levels follow a slightly different route, reaching their equilibrium values much earlier. It is noteworthy to mention that at low injection currents, the system displays population inversions not only between levels 3 and 2 but levels 3 and 1 as well. This may give rise to a new mode in the cavity although the likeliness of such an eventuality may not be very strong since in practice the two states involved are spatially well separated which reduces their radiative transition probability.

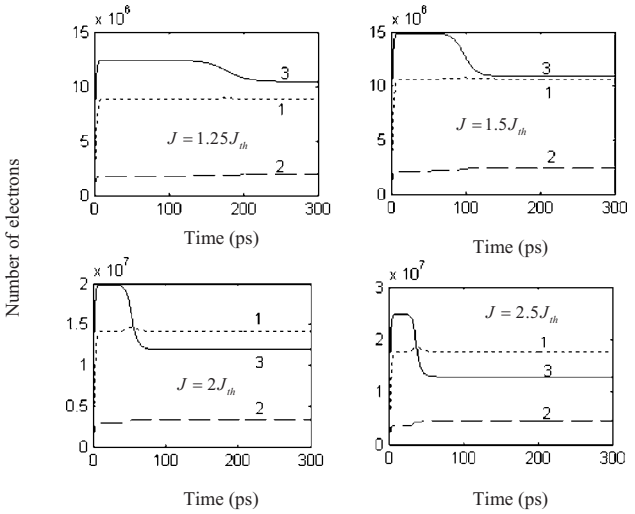

FIG. 1. Time evolution of the number of electrons in the various levels of the QC laser under different bias currents. Solid line (level 3), dashed line (level 2), and dotted line (level 1) for $\beta=2\times10^{-3}$ (Ref. 17) and $\tau_{out}=1$ ps (Ref. 13).

Figure 2 represents the time evolution of the population inversion between levels 3 and 2 normalized by the population inversion between the same levels at threshold ΔN_{th}. Also shown on the same figure is the photon number normalized by the saturation photon number $N_{ph,sat}$, the results are all obtained for an injection current $J=2.5J_{th}$. We can see that population inversion goes through different stages before reaching the stationary regime. First the injection of electrons generates an increase in the population inversion ΔN which after a time t_{th}, known as the turn-on delay time, reaches its threshold value ΔN_{th}, the cavity photon number then starts to build up from the onset of spontaneous emission processes. In the second stage, the increase of the photon number in the cavity suffers a certain delay compared to the buildup of the population inversion that follows the current injection process. During this time, the population inversion continues to increase, subsequently spurred by stimulated emission that sets in, the photon number starts to increase dramatically thus resulting in the decrease of the population inversion.

The photon number still continues to increase slightly while the population inversion decreases accordingly before the laser reaches its stable stationary regime 60 ps after the start of current injection. This behavior is similar to that observed in conventional lasers.[20] Moreover, the dynamic trajectory followed by the system to reach its state of oscillation depends crucially on the phonon scattering times and the injection current density, it also depends strongly on the spontaneous emission factor, as shown on Fig. 3, where we plot the temporal evolution of the number of photons for different values of the spontaneous emission factor β.

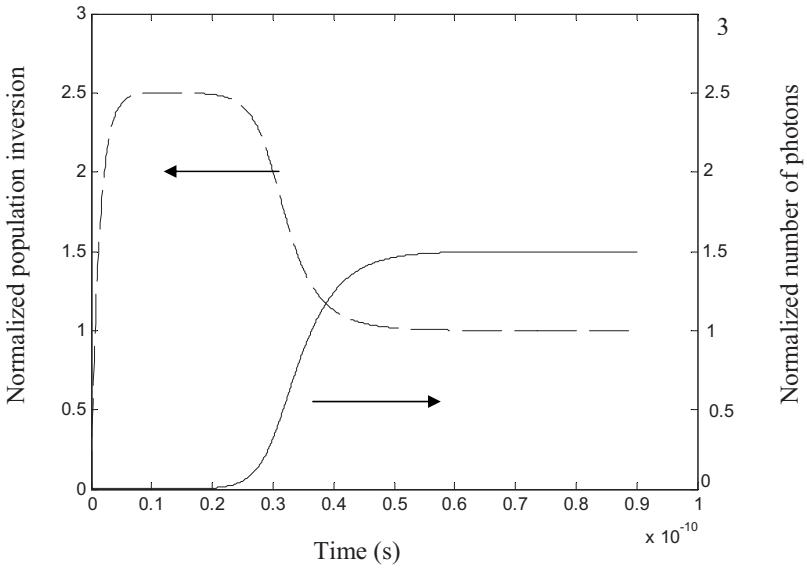

FIG. 2. Time evolution of the normalized population inversion $\Delta N/\Delta N_{\text{th}}$ (dashed line) and normalized photon number $N_{\text{ph}}/N_{\text{ph,sat}}$ (solid line) for $\beta=2\times10^{-3}$ (Ref. 17) and $\tau_{\text{out}}=1$ ps (Ref. 13).

B. Derivation of the turn-on delay and buildup times

To compute the delay time t_d that elapses between the moment the bias is applied and the time the photon number reaches 10% of its stationary value we write $t_d \approx t_{\text{th}}+\Delta t$, where t_{th} is the turn-on delay time needed for the population inversion ΔN to reach its threshold value ΔN_{th} while Δt, the buildup time, is the interval of time where the number of photons is still very small.

Note that in the interval Δt the population inversion is perfectly constant. In order to get the explicit turn-on delay time equation for the QC laser, it is convenient to determine the population inversion in terms of the QC laser parameters in absence of photons.

With the initial condition $N_3(t=0)=0$, Eq. (1a) can directly be solved yielding

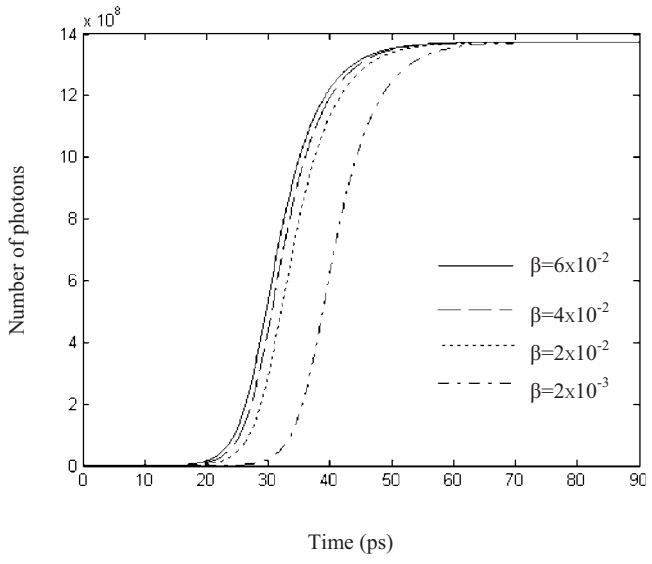

FIG. 3. Time evolution of the number of photons for different spontaneous emission factors: solid line: $\beta=6\times10^{-2}$, dashed line: $\beta=4\times10^{-2}$, dotted line: $\beta=2\times10^{-2}$, and dot-dashed line: $\beta=2\times10^{-3}$, $\tau_{\text{out}}=1$ ps (Ref. 13) and $J=2.5J_{\text{th}}$.

$$N_3(t) = WL\frac{J}{e}\tau_3(1-e^{-t/\tau_3}). \tag{16}$$

For $N_2(t)$ we use Eq. (1b) and write the solution as

$$N_2(t) = u(t)v(t). \tag{17}$$

Substituting Eq. (17) back into Eq. (1b) in the absence of any light fields and differentiating we get

$$u(t)\left(\frac{dv(t)}{dt}+\frac{v}{\tau_{21}}\right)+v(t)\frac{du(t)}{dt}=\left(\frac{1}{\tau_{32}}+\frac{1}{\tau_{\text{sp}}}\right)N_3. \tag{18}$$

The solution being unique, we first get rid of the first term in Eq. (18) by choosing $v(t)$ as

$$v(t) = e^{-t/\tau_{21}}, \tag{19}$$

then the remaining terms are easily handled and give for $u(t)$ the following expression:

$$u(t) = WL\frac{J}{e}\tau_3\left(\frac{1}{\tau_{32}}+\frac{1}{\tau_{\text{sp}}}\right)\left\{\tau_{21}e^{t/\tau_{21}}+\frac{1}{\frac{1}{\tau_3}-\frac{1}{\tau_{21}}}\times e^{-[(1/\tau_3)-(1/\tau_{21})]t}\right\}+WL\frac{J}{e}\tau_3\left(\frac{1}{\tau_{32}}+\frac{1}{\tau_{\text{sp}}}\right)c_1, \tag{20}$$

where c_1 is a constant to be determined below by the initial conditions.

Combining Eqs. (17), (19), and (20) we get the following expression for

$$N_2(t) = WL\frac{J}{e}\tau_3\left[\left(\frac{1}{\tau_{32}}+\frac{1}{\tau_{\text{sp}}}\right)\left(\tau_{21}+\frac{1}{\frac{1}{\tau_3}-\frac{1}{\tau_{21}}}e^{-t/\tau_3}\right)+\left(\frac{1}{\tau_{32}}+\frac{1}{\tau_{\text{sp}}}\right)c_1e^{-t/\tau_{21}}\right]. \tag{21}$$

The initial condition $N_2(t=0)=0$ is fulfilled if we set $c_1=-\{\tau_{21}+1/[(1/\tau_3)-(1/\tau_{21})]\}$ and the solution then becomes

$$N_2(t) = WL\frac{J}{e}\tau_3\tau_{21}\left(\frac{1}{\tau_{32}} + \frac{1}{\tau_{sp}}\right) \times \left[\frac{\frac{\tau_{21}}{\tau_3}(1 - e^{-t/\tau_{21}}) - 1 + e^{-t/\tau_3}}{\frac{\tau_{21}}{\tau_3} - 1}\right]. \quad (22)$$

From Eqs. (16) and (22) we deduce the population inversion between levels 3 and 2 as

$$\Delta N(t) = WL\frac{J}{e}\tau_3(1 - e^{-t/\tau_3})\xi_1 - WL\frac{J}{e}\tau_3(1 - e^{-t/\tau_{21}})\xi_2, \quad (23)$$

where the coefficients ξ_1 and ξ_2 are defined as

$$\xi_1 = 1 + \tau_{21}\left(\frac{1}{\tau_{32}} + \frac{1}{\tau_{sp}}\right)\frac{1}{\frac{\tau_{21}}{\tau_3} - 1} \quad (24a)$$

$$\xi_2 = \tau_{21}\left(\frac{1}{\tau_{32}} + \frac{1}{\tau_{sp}}\right)\frac{\tau_{21}}{\tau_3}\frac{1}{\frac{\tau_{21}}{\tau_3} - 1}. \quad (24b)$$

It is quite easy to see from Eq. (23) that the population inversion asymptotically approaches the value $\Delta N^{\infty} = (1 - \tau_{21}/\tau_{32} - \tau_{21}/\tau_{sp})\tau_3 J/e$. The threshold condition $\Delta N = \Delta N_{th}$ is reached after a time t_{th} solution of the equation that results by combining Eqs. (15) and (23), i.e.,

$$\frac{\xi_1 \exp\left(-\frac{t_{th}}{\tau_3}\right) - \xi_2 \exp\left(-\frac{t_{th}}{\tau_{21}}\right)}{\xi_1 - \xi_2} = 1 - J_{th}/J. \quad (25)$$

In the limiting case of a bipolar laser Eq. (25) still applies, indeed in that situation[16] $\tau_{21} \ll \tau_{32}$ and ξ_1 and ξ_2 then approach 1 and 0, respectively. One then obtains the same turn-on delay time as for a conventional laser, i.e., the already known result[16] $t_{th} = \tau_3 \ln[J/(J - J_{th})]$.

Now, in order to determine the evolution of the photon number in the interval where the oscillation develops linearly, one can replace the dynamic variables ΔN and N_3 by their respective values $\Delta N^{(0)}$ and $N_3^{(0)}$ when the number of photons in the cavity is still small, and retains the equation which results from it for the N_{ph} variable only. From Eqs. (5) and (7) we obtain for $N_3^{(0)}$ and $\Delta N^{(0)}$,

$$N_3^{(0)} = WL\frac{J}{e}\tau_3, \quad (26)$$

$$\Delta N^{(0)} = WL\frac{J}{e}\tau_3\left(1 - \frac{\tau_{21}}{\tau_{32}} - \frac{\tau_{21}}{\tau_{sp}}\right), \quad (27)$$

substituting these into Eq. (1d) and taking into account Eq. (11), we obtain the following linear first order differential equation for the photon number:

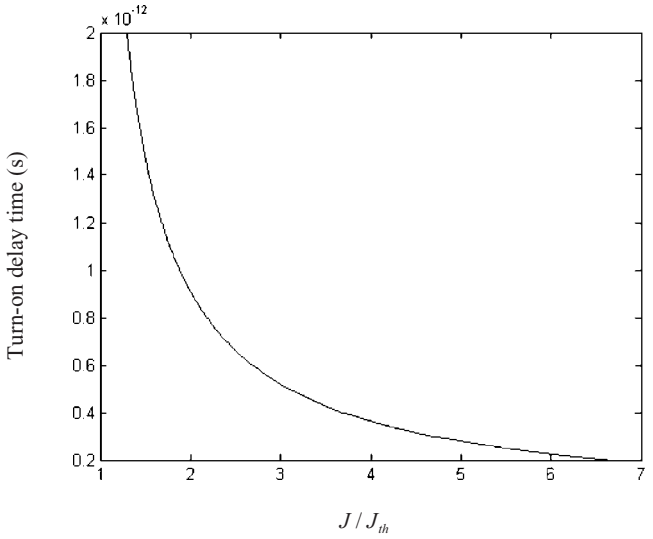

FIG. 4. Turn-on delay time variation vs normalized current density.

$$\frac{dN_{ph}}{dt} = \frac{1}{\tau_p}\left(\frac{J}{J_{th}} - 1\right)N_{ph} + WL\frac{J}{e}\tau_3\frac{N\beta}{\tau_{sp}}. \quad (28)$$

We use the following initial conditions for the intra-cavity photon number $N_{ph}(t=0) = 0$. Then Eq. (28) can be directly solved, thus

$$N_{ph}(t) = \frac{\tau_p}{\frac{J}{J_{th}} - 1}WL\tau_3\frac{N\beta}{\tau_{sp}}\frac{J}{e}(e^{(J/J_{th}-1)t/\tau_p} - 1). \quad (29)$$

Now, to compute the buildup time $\Delta t_{10\%}$, i.e., the time necessary for the laser to reach 10% of its stationary photon number, we invert Eq. (29) to get

$$\Delta t_{10\%} = \frac{\tau_p}{\frac{J}{J_{th}} - 1}\ln\left[1 + \frac{1}{10}\left(\frac{J}{J_{th}} - 1\right)^2\frac{1}{WL\frac{J}{e}\tau_3\tau_p}\frac{\tau_{sp}}{N\beta}N_{ph,sat}\right]. \quad (30)$$

From Eqs. (25) and (30) we find the connection between the delay time and such fundamental QC laser parameters as the current injection strength, the spontaneous emission factor, and the phonon scattering time, the relationship reads

$$t_d \approx t_{th} + \frac{\tau_p}{\frac{J}{J_{th}} - 1}\ln\left[1 + \frac{1}{10}\left(\frac{J}{J_{th}} - 1\right)^2\frac{1}{WL\frac{J}{e}\tau_3\tau_p}\frac{\tau_{sp}}{N\beta}N_{ph,sat}\right]. \quad (31)$$

We show in Fig. 4 the variation of the turn-on delay time as a function of the normalized current density J/J_{th} which we vary from 1 to 7, the parameters used to solve Eq. (25) being those of the previous section. It is worthwhile to stress the strong decrease of t_{th} as the injected current J increases from its minimal value J_{th} upward. In Fig. 5, the buildup time is plotted versus normalized electron current injection for three values of β, the spontaneous emission factor, and we can easily see that the buildup time is a decreasing function of both J and β.

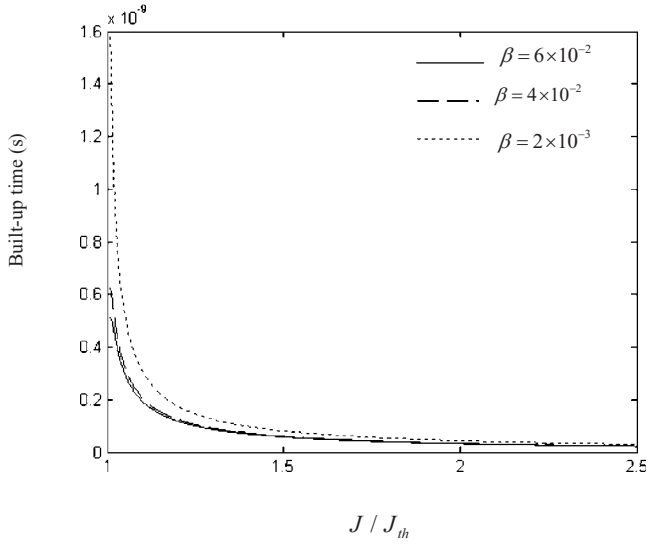

FIG. 5. Buildup time variation vs normalized current density for different values of the spontaneous emission factor: solid line: $\beta=6\times10^{-2}$, dashed line: $\beta=4\times10^{-2}$, and dotted line: $\beta=2\times10^{-3}$, $\tau_{out}=1$ ps (Ref. 13).

IV. CONCLUSION

Using a simple rate equations model, we studied the dynamics of a three-level midinfrared QC laser using realistic experimental parameters taken from the literature. The injection current is found to play a central role, dictating among other things both the values of the turn-on and delay times. We also developed an analytical scheme to derive the turn-on and delay times as functions of J and the different scattering times of the system. Our numerical results also show that the spontaneous emission factor affects the delay time quite strongly.

ACKNOWLEDGMENTS

The authors are much indebted to Dr. F. Dessenne from IEMN, Université Lille 1, France, for his generous help.

[1] J. Faist, F. Capasso, D. L. Sivco, C. Sirtori, A. L. Hutchinson, and A. Y. Cho, Science **264**, 553 (1994).
[2] H. Page, C. Becker, A. Robertson, G. Glastre, V. Ortiz, and C. Sirtori, Appl. Phys. Lett. **78**, 3529 (2001).
[3] W. H. Ng, E. A. Zibik, M. R. Soulby, L. R. Wilson, J. W. Cockburn, H. Y. Liu, M. J. Steer, and M. Hopkinson, J. Appl. Phys. **101**, 046103 (2007).
[4] G. Scamarcio, F. Capasso, C. Sirtori, J. Faist, A. L. Hutchinson, D. L. Sivco, and A. Y. Cho, Science **276**, 773 (1997).
[5] S. Anders, W. Schrenk, E. Gornik, and G. Strasser, Appl. Phys. Lett. **80**, 1864 (2002).
[6] D. Hofstetter, M. Beck, T. Aellen, and J. Faist, Appl. Phys. Lett. **78**, 396 (2001).
[7] J. Faist, M. Beck, T. Aellen, and E. Gini, Appl. Phys. Lett. **78**, 147 (2001).
[8] C. Walther, G. Scalari, J. Faist, H. Beere, and D. Ritchie, Appl. Phys. Lett. **89**, 231121 (2006).
[9] A. Hamadou, J.-L. Thobel, and S. Lamari, Opt. Commun. **281**, 5385 (2008).
[10] R. C. Iotti and F. Rossi, Phys. Rev. Lett. **87**, 146603 (2001).
[11] R. C. Iotti and F. Rossi, Physica E (Amsterdam) **13**, 715 (2002).
[12] R. C. Iotti and F. Rossi, Semicond. Sci. Technol. **19**, S323 (2004).
[13] R. C. Iotti and F. Rossi, Rep. Prog. Phys. **68**, 2533 (2005).
[14] C. Liu, R. Roy, H. D. I. Abarbanel, Z. Gills, and K. Nunes, Phys. Rev. E **55**, 6483 (1997).
[15] S. Hofling, R. Kallweit, J. Seufert, J. Koeth, J. P. Reithmaier, and A. Forchel, J. Cryst. Growth **278**, 775 (2005).
[16] K. Iizuka, *Elements of Photonics* (Wiley, New York, 2002), Vol. 2.
[17] M. Yamanishi, T. Edamura, K. Fujita, N. Akikusa, and H. Kan, IEEE J. Quantum Electron. **44**, 12 (2008).
[18] M. Troccoli, G. Scamarcio, V. Spagnolo, A. Tredicucci, C. Gmachl, F. Capasso, D. L. Sivco, A. Y. Cho, and M. Striccoli, Appl. Phys. Lett. **77**, 1088 (2000).
[19] J. T. Verdeyen, *Laser Electronics* (Prentice-Hall, Englewood Cliffs, 1995).
[20] S. E. Hodges, M. Munroe, D. Adkison, W. Gadomski, and M. G. Rayer, Opt. Lett. **17**, 931 (1992).